Photoproduction of Charged Pi Mesons from Hydrogen and Deuterium*

T. L. JENKINS, D. LUCKEY,† T. R. PALFREY,‡ AND R. R. WILSON
Cornell University, Ithaca, New York

(Received March 12, 1954)

Photoproduction cross sections of charged pi mesons from hydrogen and deuterium have been measured as a function of meson angle at gamma-ray energies of 200, 235, and 265 Mev. The angular range extends from 30° to 180° in the laboratory system. Absolute cross sections have been determined. A least-squares fit of the measured cross sections has been made to the expression $A+B\cos\theta+C\sin^2\theta$, which assumes only S and P wave scattering. The coefficients so determined are qualitatively consistent with electric and magnetic dipole absorption together with the assumption of a resonant state of angular momentum $\frac{3}{2}$ and of energy close to 300 Mev. Comparison with neutral meson production indicates some direct charged meson production in the P state.

I. INTRODUCTION

IT is of interest to study the system consisting of a single meson and a single nucleon interacting with each other. Much emphasis has been given to the scattering of mesons by protons, but the problem can also be studied from another point of view, namely, production of mesons by gamma rays incident on protons. The first photoproduction experiment from hydrogen was that of Steinberger and Bishop.[1] Other experiments are in progress or have been completed at other laboratories.[2,3]

We have measured the photoproduction cross sections of charged pi mesons from hydrogen as a function of meson angle at gamma-ray energies of 200, 235, and 265 Mev. A magnetic deflection method was used to detect the mesons and determine their energy. This obviates some of the difficulties inherent in the early measurements. In the expectation of obtaining reliable absolute cross sections, the intensity of the synchrotron beam has been carefully calibrated.

(a) Identification of the Mesons

Figure 1 shows the general arrangement of the apparatus. The gamma-ray beam of the Cornell synchroton passed through a lead collimator onto the meson producing target. A double-focusing magnet bent mesons produced at an angle θ to the gamma-ray beam through 90° to a counter telescope. The front slits of the magnet determined the angular acceptance; the rear slits and the strength of the magnetic field determined the energy of mesons counted in the telescope. An ion chamber placed behind the target monitored the gamma-ray beam. The production of mesons from hydrogen and deuterium was studied by carbon-polyethane and light-heavy water subtractions.

Mesons were identified by (1) having momenta and charge such that the magnetic field would deflect them into the counter telescope, and (2) having a sufficient range to penetrate the absorbers in the counter telescope. Protons and heavier particles of the same momentum as the mesons studied could not penetrate the absorbers. Electrons and positrons of high energy (100 to 200 Mev) would cause counts; however, they were important only at forward angles.

Some of the confirming experimental evidence that the counts were due to mesons are the following:

(1) Experimental work at Cornell using a two-magnet system and a cloud chamber showed that momentum separation at 135° gives a pure meson beam.[4]

(2) Range curves taken by placing absorbers in the counter telescope were in agreement with that expected for a meson beam with the predicted energy spread.

(3) The mesons were stopped in a carbon absorber after traversing the counter telescope. Trays of Geiger counters were located at the top and bottom of the

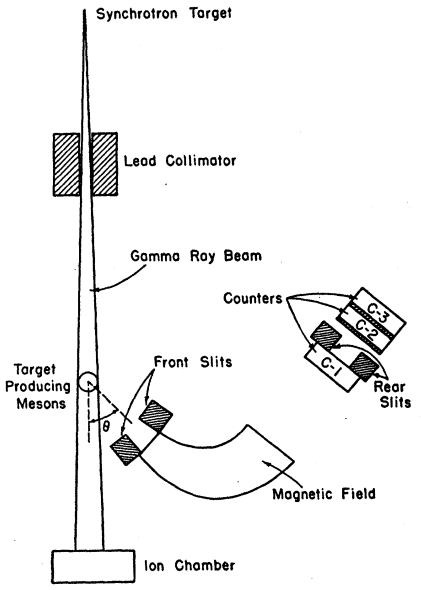

FIG. 1. Experimental layout (not to scale).

* Supported by joint program of U. S. Office of Naval Research and the U. S. Atomic Energy Commission.
† General Electric Fellow 1953.
‡ Now at Purdue University, Lafayette, Indiana.
[1] J. Steinberger and A. S. Bishop, Phys. Rev. **86**, 171 (1952).
[2] White, Jacobson, and Schulz, Phys. Rev. **88**, 836 (1952).
[3] Jarmie, Repp, and White, Phys. Rev. **91**, 1023 (1953).
[4] Camac, Corson, Littauer, Shapiro, Silverman, Wilson, and Woodward, Phys. Rev. **82**, 745 (1951).

carbon absorber, and were in delayed coincidence with the counter telescope. The stopped particles had a mean life of about 2 microseconds, in agreement with the known lifetime of the mu mesons.

(4) An excitation curve for the production of 54-Mev mesons from beryllium at 90° was made by varying the maximum energy of the synchrotron.[5] Below the threshold for meson production no counts within the statistics were observed. However, electrons and positrons with sufficient energy to traverse the system could still have been produced by the gamma-ray beam.

(b) The Magnet System

The magnet, which weighed five tons, was double-focusing with horizontal and vertical focal lengths equal ($n=\frac{1}{2}$). Mesons with energy up to 85 Mev could be bent through 90° with about a 25-cm radius of curvature. The meson-producing target was placed at the focus of the magnet so that mesons of a given momentum emerged in parallel bundles. Different momenta were bent through different angles. A lead slit about 8 cm wide and located 40 cm from the exit of the magnet selected the momenta counted by the telescope. The front slits (uranium) determined the angular acceptance and limited the meson trajectories to the usable part of the field. All the slits, the counter telescope, and the target holder were mounted rigidly to the magnet yoke so that the complete system remained identical when the magnet was moved from angle to angle.

(c) The Counter Telescope

The counter telescope consisted of three proportional counters of square cross section 2 in.×2 in. and 6 in. long; they were filled at atmospheric pressure with a mixture of 5 percent carbon dioxide in argon. The walls through which the mesons passed were 0.003-in. brass. Absorbers were placed between the counter walls to reduce the background and to set a lower limit on the range of the particles counted. For most of the measurements the absorber between counters C-1 and C-2 was $\frac{1}{16}$-in. Lucite, and the absorber between C-2 and C-3 was $\frac{1}{16}$-in. lead. Proportional counters were chosen in preference to scintillation counters because of their lower response to the stray neutrons in the synchrotron room. No use was made of the proportional properties in identifying the mesons. Proportional counters also have the advantage of no dead time.

(d) Electronics

Pulses from the proportional counters were preamplified and sent via White cathode followers to the detection room where 204-B Atomic amplifiers were used. Shaped pulses were fed into a Rossi coincidence circuit which had a resolving time of about 0.5 microsecond. Those input pulses which caused coincidences were watched by a pulse-height analyzer; the gain of the amplifiers were adjusted so that the pulses causing the coincidences were well above the discrimination level.

(e) Targets

The targets used were cylinders 1 inch in diameter with their axes perpendicular to the plane of the pole pieces and the gamma-ray beam. If the beam were uniform over the target, then the target geometry would be independent of the angle of the magnet system with respect to the gamma-ray beam. Various special targets were constructed for certain aspects of the experiment. These included a carbon target designed to produce as many electrons as the polyethane target (used at forward angles), a carbon target having the same average stopping power as the polyethane target (used at low meson energies), and a small polyethane target $\frac{1}{2}$ in. high and $\frac{1}{2}$ in. in diameter (used to check the calibration of the solid angle).

(f) The Gamma-Ray Beam

The gamma-ray beam used in this experiment was the bremsstrahlung from 304–309 Mev electrons striking a 0.040-inch tungsten target in the Cornell synchrotron. The resulting spectrum of gamma rays has been measured at Cornell by J. W. DeWire and in the energy region of this experiment was not significantly different from the Bethe-Heitler spectrum. The calculations were made assuming a Bethe-Heitler spectrum. The gamma-ray beam was spread in time by turning off the rf slowly, so that the period of expulsion was 1.5 milliseconds centered about the peak of the magnetic cycle. Electrons striking the target lay in the energy range from 304 to 309 Mev, with an average energy of 307 Mev. The gamma-ray beam was collimated by a $\frac{1}{2}$ in.×$\frac{1}{2}$ in. square slit of lead located at a distance of 1.5 meters from the target. For some of the angles, additional collimation was used behind this collimator. The measurements at 180° were made using a $\frac{3}{8}$ in. ×$\frac{1}{2}$ in. collimator in order that the beam would not hit the poles of the magnet. The beam was monitored by a thick-walled (copper) air-filled ionization chamber (standard at Cornell) located behind the meson producing target. The chamber was calibrated with the pair spectrometer and by use of shower curves in aluminum.

II. CALCULATION OF THE CROSS SECTION

(a) Expression for the Cross Section

Because we were studying a two-body process, the measurement of the energy and angle of the meson uniquely specified the reaction including the gamma-ray energy. The computation of a cross section from the observed counting rate required a knowledge of (1) the

[5] D. Luckey, Phys. Rev. **90**, 711 (1953).

gamma-ray beam, (2) the magnet system, (3) the losses due to decay in flight of pi mesons, (4) the kinematics of the reaction, and (5) the structure of the target. The properties of the gamma-ray beam which had to be known were the spatial distribution of the intensity across the beam, the energy spectrum of the gamma rays and the intensity. The intensity was measured by the monitoring ionization chamber. The magnet system can be described by the meson energy which is a function of the magnet current and the solid angle which is a function of meson energy at a fixed magnet current. The structure of the target had to be known both physically and chemically. From the definition of differential cross section we have that the number of mesons, N_π, produced is given by

$$N_\pi = Nt' \int_\nu \left(\frac{d\sigma}{d\Omega}\right) \Omega(\nu) N(\nu) d\nu,$$

where N is the number of target nuclei, t' is the effective target thickness, $d\sigma/d\Omega$ is the differential cross section, $\Omega(\nu)$ is the solid angle, and $N(\nu)d\nu$ is the energy spectrum of the gamma rays.

In practice the integration is done over meson energy T rather than ν. Ω is then a property of the magnet system which was measured. The number of gamma rays was obtained from the bremsstrahlung spectrum and the charge collected on the ion chamber. The effective thickness of the target was calculated from the spatial distribution of the beam and the geometry of the target and experimentally measured by changing the target size. The effective thickness differs by about 10 percent from that one would calculate geometrically. N_π is obtained by correcting the counting rate for the various losses. The differential cross section was then obtained and, via the known kinematics, transformed to the center-of-mass system.

(b) Corrections to the Counting Rates

The following corrections were applied to the observed counting rates to get N_π:

(1) π-μ decay in flight;
(2) scattering out of the meson beam in the various absorbers and air;
(3) nuclear absorption of the pi mesons in various materials;
(4) penetration of the rear slit;
(5) high-energy electrons at forward angles;
(6) absorbers in front of the magnet;
(7) distortion of the low-energy spectrum of mesons due to scattering of higher-energy mesons in the front slits;
(8) misalignment of the gamma-ray beam with respect to the target.

The distance from the meson-producing target to the counter telescope was 100 cm. Thus ten to twenty

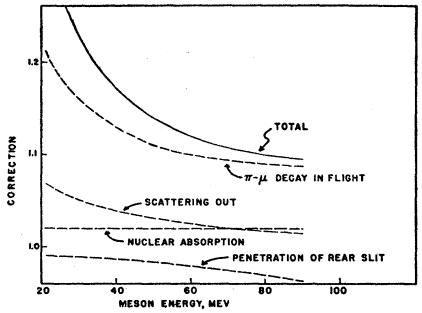

FIG. 2. Corrections to counting rate as a function of meson kinetic energy in the magnet.

percent, depending on the energy, of the mesons would decay in flight. Most of the residual μ mesons could not traverse the telescope because of the good vertical geometry. The actual correction as a function of meson energy is shown in Fig. 2 (this includes the small number of μ mesons which could still penetrate the counter).

Nuclear absorption is a small correction because of the thinness of the absorber placed in the meson beam. The absorption cross section was taken as that corresponding to a radius of $1.4\times10^{-13}A^{\frac{1}{3}}$ cm. The correction was two percent, of which about half was due to absorption in the meson-producing target and half due to lead absorber between C-2 and C-3.

Multiple scattering by the various materials in the meson path could cause counting losses because of the good vertical geometry of the telescope. A correction of between two and five percent was determined by calculation. The calculation was checked by placing a scatterer directly in front of the counter telescope and then observing the decrease of the coincidence counting rate. Figure 2 shows the variation of this small correction with meson energy.

The correction for penetration of the slit edges by the mesons amounted to about three percent at most, and is shown in Fig. 2.

Table I summarizes the corrections which depend upon the energy of the meson and shows the estimated errors in these corrections.

At forward angles it was necessary to make a correction for scattered electrons. At 30° a correction of 13 percent to the 200-Mev photon and 5 percent to the 235-Mev point was determined experimentally. This was done by performing the following auxiliary experi-

TABLE I. The magnitudes and errors of those corrections which depend upon the meson kinetic energy.

Correction factor	Meson kinetic energy 30 Mev	50 Mev	80 Mev
Decay	1.16±0.02	1.11±0.01	1.09±0.01
Nuclear absorption	1.02±0.01	1.02±0.01	1.02±0.01
Multiple scattering	1.05±0.02	1.03±0.01	1.02±0.01
Slit penetration	0.99±0.01	0.98±0.02	0.97±0.02
Total	1.23±0.03	1.14±0.03	1.10±0.03

TABLE II. The results of solid-angle measurements at different magnetic field intensities.

T (Mev)	$\int\Omega(T)dT$ (Mev-sterad)
31	0.103±0.007
54	0.151±0.008
84	0.189±0.009

TABLE III. Experimental results for the reaction $\gamma+p\rightarrow\pi^+ +n$ for 200-Mev gamma rays.

θ_{cm}	Corrected center-of-mass cross section (μb/sterad)	Statistical error (%)	Corr. for loss	Special corrections
39	7.0±1.1	13.5	1.13	1.13[a]
59	10.5±1.2	7.7	1.15	1.02[a]
75	9.5±1.3	10.6	1.17	
107	9.6±1.3	10.2	1.22	
135	11.9±1.9	13.7	1.28	

[a] Electrons.

ments: (1) A search for negative particles being produced from hydrogen was made; this was also done at 90° and no negative mesons were found. Hence, the negative rate from hydrogen at 30° could be expected to estimate the number of scattered electrons. (2) By placing a fourth counter behind the counter telescope with sufficient absorber in front of it to stop the meson beam, electrons could be detected in this counter either directly or through the production of a small shower. The efficiency of the electron counter, about 30 percent, was calibrated using a high-Z target which essentially produces only electrons. (3) By varying the thickness of the target and looking for a nonlinearity in the counting rate, the number of electrons can be estimated since the electron rate will vary as the square of the target thickness. An attempt was made to move to 15° in the laboratory, but the electron rate was too large for the subtraction technique.

For the highest photon energy studied and at forward angles, the meson energy was greater than could be detected by the magnet-counter system. Aluminum absorbers were placed in front of the magnet so that the energy spectrum of the incident mesons would be shifted downward into the range of the magnet. A total correction of between seventeen and sixty percent was necessary due to (a) the nonlinearity of the range-energy curve, (b) nuclear absorption, and (c) conversion of gamma rays produced by neutral mesons into electrons which could then be counted. In order to test the absorber method, the same mean energy of mesons was studied at two different magnet current settings, with and without an absorber. When the above corrections were applied, the results agreed within the statistics.

(c) Solid Angle Measurements and Resolution

The solid angle and resolution of the magnet system were studied and calibrated by means of the current carrying wire technique. A small mirror was mounted on the wire near the target holder. The mirror reflected a beam of light to a screen; hence measuring the relative angle between the mirror and the light beam. With the current and tension adjusted to correspond to a given meson energy T, the wire was positioned so that it just grazed one of the defining apertures, and the position of the light beam recorded. The wire was then moved so that it grazed some other part of the aperture. In this manner a projection of the aperture corresponding to the given energy was traced out on the screen. The solid angle $\Omega(T)$ can then be calculated from a knowledge of the geometry of the screen and light source. With a given magnetic field the apertures were traced out for many different energies which could pass through the system. The integral $\int\Omega(T)dT$ could then be computed.

To reach high meson energies, it was necessary to saturate the iron of the magnet. The main effect of the saturation is a loss of vertical focusing. At high current, the integrated energy solid angle falls below that predicted for an ideal magnet. Solid angle measurements were made at magnet currents corresponding to mean meson energies of 31, 54, and 84 Mev. The results of these measurements and their estimated accuracy are shown in Table II. The integrated solid angles at other meson energies were determined by interpolation based on a knowledge of the point of saturation and the behavior of an ideal magnet.

The band of gamma-ray energies accepted by the magnet system is relatively independent of the experimental angle. The full widths at half-maximum were

TABLE IV. Experimental results for the reaction $\gamma+p\rightarrow\pi^+ +n$ for 235-Mev gamma rays.

θ_{cm}	Corrected center-of-mass cross section (μb/sterad)	Statistical error (%)	Corr. for loss	Special corrections
39	9.7±1.1	7.6	1.10	1.05[a]
59	11.6±1.0	4.3	1.10	
75	13.3±1.2	4.8	1.11	
107	14.6±1.3	3.3	1.13	
135	14.8±1.4	5.0	1.18	
161	15.8±1.7	7.0	1.21	
180	11.3±1.2	7.2	1.22	

[a] Electron contamination.

TABLE V. Experimental results for the reaction $\gamma+p\rightarrow\pi^+ +n$ for 265-Mev gamma rays.

θ_{cm}	Corrected center-of-mass cross section (μb/sterad)	Statistical error (%)	Corr. for loss in magnet	Absorber correc.
39	8.0±1.0	8.0	1.10	1.61
59	11.6±1.1	5.6	1.10	1.30
75	18.2±1.7	4.7	1.10	1.17
107	19.9±1.7	3.4	1.11	
135	19.9±1.8	5.2	1.13	
161	17.0±2.4	11.7	1.15	
180	14.8±1.5	5.8	1.17	

estimated to be 15 Mev at 200 Mev, 22 Mev at 235 Mev, and 30 Mev at 265 Mev. The extreme limits which can contribute were estimated to be 200±10, 235±15, and 265±20 Mev. In arriving at the above estimates, the broading of the intrinsic magnetic resolution by the finite size of the target and the energy loss therein has been included.

III. EXPERIMENTAL RESULTS

(a) Photoproduction from Hydrogen

Tables III, IV, and V give our results for the cross sections for the reaction $\gamma+p\rightarrow\pi^+ +n$ at gamma-ray energies of 200, 235, and 265 Mev. The tables also show the statistical error in the counting rate and the magnitudes of the various corrections applied. The errors given on the cross sections include the statistical counting rate error plus estimates of the errors in the corrections and in the determination of the solid angle.

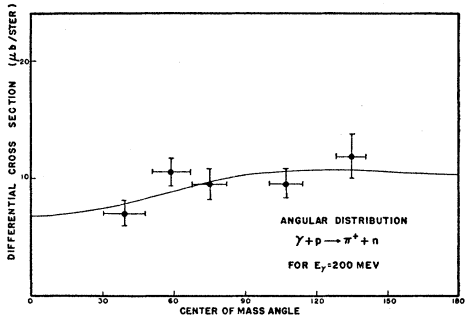

FIG. 3. Angular distribution at $E_\gamma=200$ Mev.

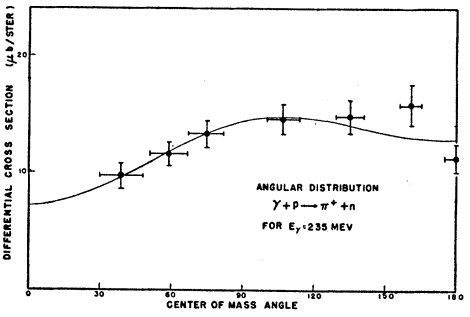

FIG. 4. Angular distribution at $E_\gamma=235$ Mev.

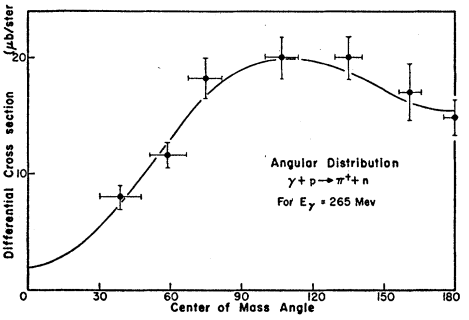

FIG. 5. Angular distribution at $E_\gamma=265$ Mev.

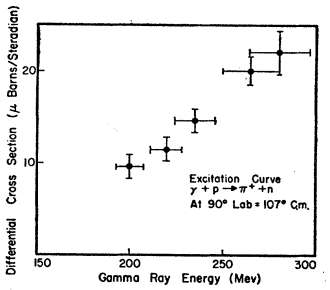

FIG. 6. Excitation curve for $\gamma+p\rightarrow\pi^+ +n$ at 90° lab $=107°$ c.m.

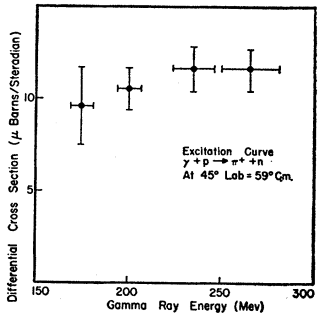

FIG. 7. Excitation curve for $\gamma+p\rightarrow\pi^+ +n$ at 45° lab $=59°$ c.m.

In addition, the absolute scale of the cross section may be in error because of uncertainties in the calibration of the gamma-ray beam and other systematic errors.

The angular distributions are shown in Figs. 3, 4, and 5. Excitation functions at 45° and 90° are shown in Figs. 6 and 7.

Table VI shows the total cross sections for the reaction at the various energies.

(b) Photoproduction from Deuterium

Table VII shows the experimental ratios of charged pi-meson production from deuterium to the production from hydrogen.

(c) Search for Negative Mesons from Hydrogen

A special search was made for negative mesons produced from hydrogen with a bremsstrahlung spectrum of maximum energy 310 Mev. The experiment was performed at 90° in the laboratory system with the magnet set to accept 34-Mev mesons. Special large targets were constructed to increase the counting rates. To check that the targets contained the same amount of carbon the negative rate was also measured for 78-Mev mesons. In both cases no negative particles were detected from hydrogen within the counting statistics. The positive rate from hydrogen was also measured from the same target. The negative rate was 1 percent±4 percent of the positive rate for 34-Mev mesons at 90°.

IV. DISCUSSION

Arbitrarily assuming that only S and P waves contribute to the cross section in this energy region, one can write

$$\sigma'=A+B\cos\theta+C\sin^2\theta.$$

TABLE VI. Total cross sections for the reaction $\gamma+p\rightarrow\pi^+ +n$.

E (Mev)	$\sigma_{\text{total}}(10^{-28}$ cm$^2)$
200	1.22±0.09
235	1.64±0.06
265	1.96±0.08

TABLE VII. Experimental results for charged meson production from deuterium.

θ_{lab}	Mev	π^+ from deuterium / π^+ from hydrogen	π^- from deuterium / π^+ from hydrogen	(π^-/π^+) from deuterium
45°±7°	48	1.07±0.14	0.57±0.09	0.54±0.11
	78	0.77±0.13	0.76±0.06	0.98±0.19
90°±7°	34	0.73±0.14	0.77±0.16	1.06±0.32
	46		0.81±0.17	
	54	0.72±0.09	1.07±0.15	1.49±0.25
	64		0.74±0.09	
	72		0.69±0.06	
	84	0.58±0.13	0.76±0.09	1.31±0.34
180°±7°	34		0.98±0.27	
	46	0.92±0.18	0.87±0.19	0.85±0.26

The cross sections given in Table III, IV, and V were least squares fitted to the above expression. The values of the coefficients so obtained are given together with their standard deviations in Table VIII. The errors in the coefficients are correlated. That the data are well fitted can be seen in Figs. 3, 4, and 5.

Following Brueckner and Watson[6] and Feld,[7] one can write the following relationships between the above coefficients and the amplitudes a and b (respectively for electric dipole and magnetic dipole absorption), assuming that the p-wave contribution to the process goes through a definite state of total angular momentum $\frac{3}{2}$:

$$A=a^2+b^2,\quad B=2ab\cos\phi,\quad C=\tfrac{3}{2}b^2.$$

ϕ is the phase angle between the S and P waves. Table IX gives the values of a^2, b^2, and ϕ, together with their standard deviations.

The dependence of a^2 with increasing energy is reminiscent of other S-wave dipole transitions such as the magnetic dipole photodisintegration of the deuteron. The amplitude of the P wave increases very rapidly with energy and invites comparison with the neutral photomeson production data. If one assumes that both neutral and charged photoproduction in the P state go through the same state of total angular momentum, then one must allow another internal degree of freedom to determine the branching ratio. Brueckner and Watson and Feld have assigned an isotopic spin of $\frac{3}{2}$ to the state, in which case it follows that the neutral production should be twice the charged production in the P-wave state. It appears that the P-wave part of neutral production is equal or less than the charged production.[8–10] This indicates that the above assumptions are wrong. Perhaps this implies that electric quadrupole absorption is also important in the process. Chew[11] has indicated, that there can be a direct interaction in the P state in the case of charged production which may not occur in neutral production. This might account for the discrepancy in the branching ratio. The behavior of ϕ with energy is just that expected if there were a resonant state at about 300 Mev. Thus, ϕ should change by 180° in going from below the resonant energy to above it, if the phase of the S wave does not change too rapidly. It thus appears that our data are consistent with the existence of a single resonant state of angular momentum $\frac{3}{2}$ and isotopic spin $\frac{3}{2}$.

We are in excellent agreement with other laboratories where comparison with our results can be made.

TABLE VIII. Values of coefficients in least-squares fit of form $\sigma'=A+B\cos\theta+C\sin^2\theta$.

E (Mev)	A	B	C
200	8.5±2.2	−1.9±1.3	1.8±2.9
235	10.0±1.0	−2.8±0.8	4.5±1.6
265	8.7±1.1	−6.9±0.9	10.4±2.0

TABLE IX. Values of coefficients in Feld's theory.

E (Mev)	a^2	b^2	ϕ
200	7.4±4.2	1.2±1.9	109°±20°
235	7.0±2.1	3.0±1.1	108°± 5°
265	1.7±2.4	6.9±1.3	175°±25°

[6] K. A. Brueckner and K. M. Watson, Phys. Rev. **86**, 923 (1952).
[7] B. T. Feld, Phys. Rev. **89**, 330 (1953).
[8] Jenkins, Luckey, and Wilson, Bull. Am. Phys. Soc. **29**, No. 1, 18 (1954).
[9] A. Silverman and M. Stearns, Phys. Rev. **88**, 1225 (1952).
[10] Goldschmidt-Clermont, Osborne, and Scott, Phys. Rev. **89**, 329 (1953).
[11] G. Chew (private communication).